

## Effect of the Concentration Polarization on the Hydrogen Permeation through Pd-based membranes

A. Caravella<sup>1,2</sup>, G. Barbieri<sup>2</sup>, E. Drioli<sup>1,2</sup>

<sup>1</sup>Dept. of Chemical and Materials Engineering, University of Calabria  
Via P. Bucci, Cubo 44/A, 87036, Rende (CS), Italy.

<sup>2</sup>Institute on Membrane Technology, ITM-CNR, c/o University of Calabria  
Via P. Bucci, Cubo 17/C, 87036, Rende (CS), Italy.

The aim of this investigation was analyzing the influence of the concentration polarization on the performances of Pd-alloy membranes involved in hydrogen separation processes. The analysis was carried out by means of a model already introduced and validated elsewhere (Caravella et al., 2008). The influence of several different operating conditions was considered: up-stream hydrogen molar fraction, total pressure of upstream and down-stream, temperature, membrane thickness and upstream fluid-dynamic conditions, considering the presence of a multicomponent gaseous mixture in the upstream side and pure hydrogen in the downstream one. After investigating the role of the permeance and permeating flux on the concentration polarization, the so-called "polarization maps" were drawn, being diagrams where the overall results of the investigation were shown. In these maps the polarization level is directly measurable in dependence on the characteristic of the system, providing a useful tool to choose the best working conditions for the membrane.

### 1. Introduction

With the improvements of membrane fabrication technology, very thin selective layers have been progressively ( $< 5\mu\text{m}$  ca) produced, even for metallic membranes (e.g. Mejdell et al., 2008; Mekonnen et al., 2008; Peters et al., 2008). Among these, the Pd-alloy ones play an important role thanks to their peculiarity to be permeable only towards hydrogen. If, on one hand, the reduction of selective layer thickness determines an increasing transmembrane flux owing to a decrease of the selective layer resistance, on the other hand the external mass transfer can become one of the slowest elementary steps which the whole permeation process is composed of, causing the concentration polarization to significantly affect the membrane performances. In these conditions, the Sieverts' law (valid just in case of intra-lattice hydrogen diffusion to be the only rate-determining step) cannot be used for modelling the hydrogen permeation through Pd-based selective layer and, therefore, a systematic approach to evaluate the polarization level is necessary for the correct design of the membrane-based separation equipments. The aim of this study is justly to introduce such an approach, using a complex model already introduced and validated elsewhere (Caravella et al., 2008). The polarization

level will be evaluated by means of an appropriately defined Concentration Polarization Coefficient (CPC, see Section 3), which will be represented in some "*polarization maps*" introduced in the incoming analysis.

## 2. Description of the system

The system considered in this study is sketched in Figure 1. Figure 1b represents the schematization of the possible situations occurring in the generic axial position of a tube-in-tube permeator (Figure 1a) during a hydrogen purification/supply process. On the upstream side ("mixture side") a multicomponent gas mixture is considered, whilst only hydrogen is present on the other side ("pure H<sub>2</sub> side"). The topic phenomenon of this analysis, i.e. the concentration polarization, occurs only in the mixture side due to the presence of the other non-permeating gases, whereas there is no permeation driving force drop in the pure H<sub>2</sub> side. Both forward (mixture→pure H<sub>2</sub>) and backward (pure H<sub>2</sub>→mixture) permeations are studied, in order to analyze the system behaviour as purifier as well as hydrogen supplier to mixture. The path of permeance and CPC from high to low hydrogen composition will be indicated in the coming figures in terms of polarization effect and membrane performance changes.

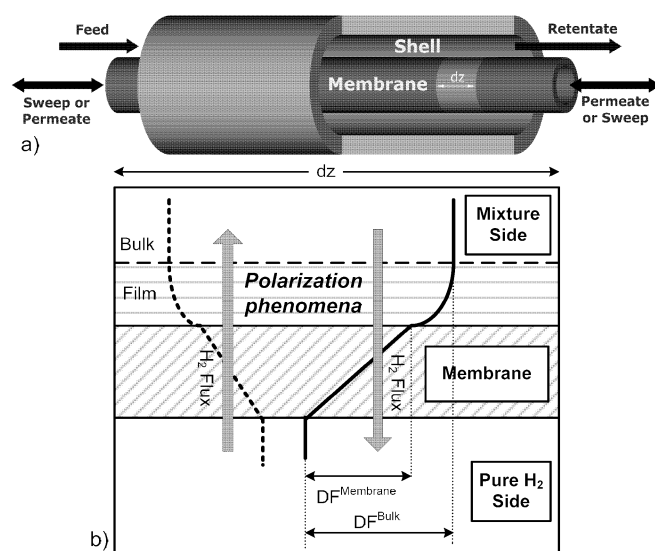


Figure 1. Schematic representation of hydrogen permeation (b) in a generic point of a tube-in-tube membrane permeator (a). The continuous and dashed lines indicate the forward and backward permeation case, respectively.

These paths are named here as "*separation paths*" and will be discussed in more details in the incoming analysis. The operating conditions considered here for the system and the mixture composition (six components) are reported in Table 1, where it is shown that a Reynolds' number of 1000 is considered (laminar conditions). For a similar system, other fluid-dynamic conditions were already studied in details elsewhere (Caravella et al., 2009).

Table 1. Operating conditions considered for the analysis.

Side	Molar Fraction, -						Total Pressure, kPa	Reynolds' number
	H <sub>2</sub>	N <sub>2</sub>	O <sub>2</sub>	CO <sub>2</sub>	H <sub>2</sub> O	CH <sub>4</sub>		
Mixture	{0 ... 1}	0.2 ... 0 (for each inert species)					{400 ... 1000}	≈ 1000
Pure H <sub>2</sub>	1	Not present					200	Not influent
Temperatures, °C = {300, 350, 400, 450, 500}								
Membrane Thicknesses, μm = {5, 15, 50, 100}								

### 3. Concentration Polarization Coefficient

In the present study, the Concentration Polarization Coefficient (*CPC*) is defined according with Eq.1-5, where  $\pi^{Membrane}$ ,  $\pi^{Bulk}$  and  $DF^{Bulk}$  are the membrane and bulk permeance and the permeation driving force of bulk, respectively.

$$H_2 \text{ Flux (Elementary Steps)} = (1 - CPC) \pi^{Membrane} DF^{Bulk} \quad (1)$$

$$CPC = 1 - \frac{H_2 \text{ Flux (Elementary Steps)}}{\pi^{Membrane} DF^{Bulk}}, \quad DF^{Bulk} = \Delta \sqrt{P_{H_2}} \Big|^{Bulk} \quad (2, 3)$$

$$\pi^{Bulk} = \frac{H_2 \text{ Flux (Elementary Steps)}}{DF^{Bulk}} \Rightarrow, \quad CPC = 1 - \frac{\pi^{Bulk}}{\pi^{Membrane}} \quad (4, 5)$$

The hydrogen permeating flux (left hand side of Eq.1) is evaluated by means of a complex model developed elsewhere (Caravella et al., 2008) accounting for all the permeation elementary steps, whilst the expression on the right hand side of Eq.1 is a general expression involving a general driving force, which in this case has been chosen to be the Sieverts' one. The usefulness of the so-defined *CPC* consists in the fact that in this way it is possible to express the flux in terms of directly measurable quantities, i.e.,  $\pi^{Membrane}$  and  $DF^{Bulk}$ , whose values can be obtained by pure-H<sub>2</sub> tests ( $\pi^{Membrane}$ ) and from the operating conditions ( $DF^{Bulk}$ ). The flux calculation can be carried out by the above-mentioned model once the external operating conditions are set. The bulk permeance  $\pi^{Bulk}$  can be evaluated as well. According with Eq.5, when polarization is negligible, the value of *CPC* is next to zero ( $\pi^{Membrane} \cong \pi^{Bulk}$ ), whereas it goes towards one in conditions of maximum polarization.

### 4. Results and discussion

In Figure 2 the bulk and membrane permeances (below) and the hydrogen flux (above) are shown as functions of hydrogen molar fraction in mixture at different membrane thicknesses at a mixture total pressure of 1000 kPa. In both plots, the line (dashed vertical one) corresponding to a null driving force is also indicated. At the left of this line back-permeation occurs and the system act as hydrogen supplier, since hydrogen partial pressure in mixture is lower than the one in the pure hydrogen side (200 kPa).

Furthermore, the here-called "separation paths" (indicated with thicker arrows following the flux and permeance curves) are also shown for the forward (e.g. from 0.9 to 0.4) and backward (e.g. from 0 to 0.1) permeation. Considering the permeances, it has to be noticed that  $\pi^{Membrane}$  (horizontal superior boundary of each coloured part) is a membrane intrinsic properties and, therefore, does not depend on the external conditions of the mixture except the temperature. Hence, it shows a constant behaviour in the figure. On the contrary,  $\pi^{Bulk}$  takes into account all the transport phenomena occurring out of the membrane and, for this reason, is significantly reduced by the external mass transfer, which is in turn influenced by the mixture composition. At the unitary value of hydrogen molar fraction the two permeances are equal, but, as the influence of the other inert species increases, a gap between them is generated, which is related to the concentration polarization level in the process.

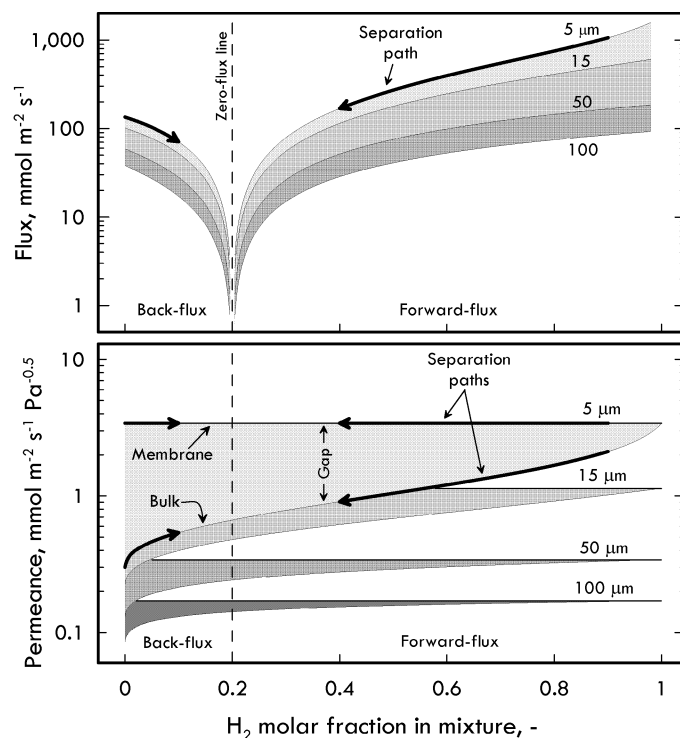


Figure 2.  $H_2$  permeating flux and both permeances (of bulk and membrane) as functions of  $H_2$  molar fraction at different membrane thicknesses.  $T=500^\circ C$ ,  $P^{Mixture} = 1000 \text{ kPa}$ .

Following the curves at  $5 \mu\text{m}$  in forward permeation case from higher to lower molar fraction, during the separation process both the flux and bulk permeance decreases in the same qualitative manner for high molar fractions. However, their behaviours are different, as they approach to the zero-flux point. In particular, the bulk permeance tends to assume a well determined finite value, being the same one found for the back-flux case, whereas the flux tends naturally to zero. The most important aspect of this

fact is that, for a certain membrane, it is possible to identify two different characteristic permeances: 1) the already known intrinsic membrane permeance  $\pi^{Membrane}$  and 2) the here-called "zero-flux bulk permeance"  $\pi_0^{Bulk}$ , which can be evaluated from the external condition of mixture. At higher membrane thicknesses the situation is qualitatively similar, but the gap between the two permeances is progressively reduced owing to the major influence of the hydrogen diffusion in the metal selective layer. The physical meaning of this important aspect is that a membrane has two characteristic values of permeance. The first one, obtainable in pure hydrogen permeation test, is a property of the only membrane and represents the maximum permeance reachable, whilst the second one is a characteristic proper of both membrane and fluid-dynamic conditions.

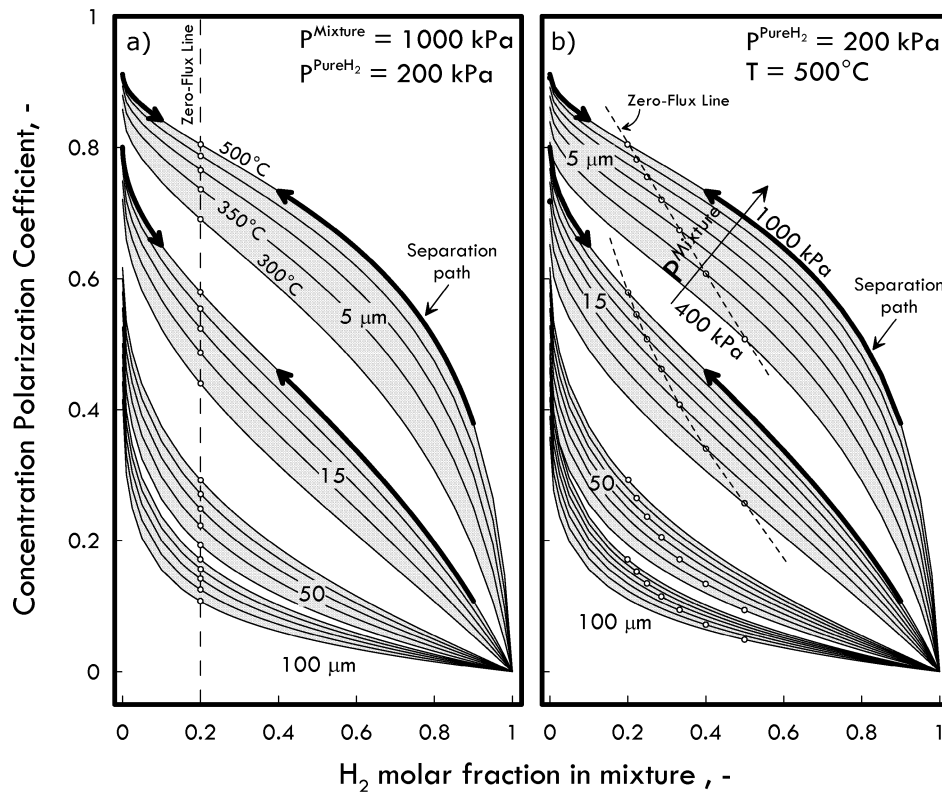


Figure 3. CPC as a function of the  $H_2$  molar fraction for different membrane thicknesses and a) temperatures at  $P^{Mixture} = 1000$  kPa, b) total pressures of mixture at  $500^\circ\text{C}$ .

In the incoming figures, *CPC* is analyzed as function of several operating conditions (temperature, hydrogen molar fraction in mixture and mixture total pressure) and membrane thicknesses in laminar flow regime ( $Re \approx 1000$ ). The so-obtained results are presented in two "polarization maps" (Figure 3a and 3b) showing the *CPC* behaviour as a function of hydrogen molar fraction and useful to determine the polarization level in different situations. Analogously to Figure 2, also in Figure 3 the separation paths are indicated with thicker arrowed curves. Considering the curve in Figure 3a at  $500^\circ\text{C}$  and

5  $\mu\text{m}$ , *CPC* increases significantly from a unitary molar fraction to lower values. This behaviour can be explained by means of the following considerations: examining progressively higher hydrogen molar fractions, the driving force becomes higher as well as the permeating flux. This effect would tend to increase the polarization due to the high transmembrane transfer rate. However, at the same time, the presence of the inert species is reduced and this fact causes the polarization to decrease. The overall result of these two contrasting factors is that *CPC* is affected by the inert presence much more than by the permeation rate. The effect of the permeation rate on *CPC* is directly recognizable considering the system behaviour at a certain value of hydrogen molar fraction at progressively higher temperatures (Figure 3a) and/or total pressures of mixture (Figure 3b). In fact, in both these cases *CPC* increases because of the flux increase, owing to the higher temperature and driving force, respectively. As above mentioned, at higher membrane thicknesses the situation is analogous, but the polarization is progressively lower since the resistance in the selective layer increases its influence on the permeation process.

## 5. Conclusions

In this study the concentration polarization was investigated in hydrogen permeation through Pd-alloy membranes. First, the effect of the permeating flux and both membrane and bulk permeances on the polarization was considered. Then, the behaviour of the concentration polarization coefficient was analyzed in different operating conditions, showing that it decreases with hydrogen molar fraction in mixture and membrane thickness, whereas increases with temperature and upstream total pressure. The methodology proposed in the present paper allows the polarization level to be quantitatively evaluated in form of the here-called "*polarization maps*", which can be built once external conditions and membrane permeation parameters are known. In this way, it is possible to avoid as much as possible the inefficiencies of a membrane separation process by taking correctly into account the polarization effects.

## Acknowledgments

The project "FIRB-CAMERE (RBNE03JCR5) co-funded by "Ministero dell'Università e della Ricerca" (MUR, Italy) is gratefully acknowledged for co-funding this research.

## References

- Caravella A., Barbieri G. and Drioli E., 2009. Concentration polarization analysis in self-supported Pd-based membranes. Separation Purification Technology. In press.
- Caravella A., Barbieri G. and Drioli E., 2008. Chem. Eng. Sci., 63, 2149.
- Mejdell A.L., Klette H., Ramachandran A., Borg A. and Bredesen R., 2008. J. Mem. Sci., 307, 96-104.
- Mekonnen W., Arstad B., Klette H., Walmsley J.C., Bredesen R., Venvik H. and Holmestad R., 2008. J. Mem. Sci., 310, 337-348.
- Peters T.A., Stange M., Klette H. and Bredesen R., 2008. J. Mem. Sci., 316, 119-127.